arXiv:1211.2790v1 [cond-mat.str-el] 12 Nov 2012

Theory of Quantum Phase Transition in Iron-based Superconductor with Half-Dirac Nodal Electron Fermi Surface

Imam Makhfudz
Department of Physics and Astronomy, Johns Hopkins University,
3400 North Charles Street, Baltimore, Maryland 21218, USA

The quantum phase transition in iron-based superconductors with 'half-Dirac' node at the electron Fermi surface is a $T = 0$ structural phase transition described in terms of nematic order. An effective low energy theory that describes half-Dirac nodal Fermions and their coupling to Ising nematic order that describes the phase transition is analyzed using renormalization group(RG) study of the large-N_f version of the theory. The inherent absence of Lorentz invariance of the theory leads to RG flow structure where the velocities v_F and v_Δ at the paired half-Dirac nodes ($1\bar{1}$ and $2\bar{2}$) in general flow differently under RG, implying that the nodal electron gap is deformed and the C_4 symmetry is broken, explaining the structural (orthogonal to orthorhombic) phase transition at the quantum critical point(QCP). The theory has Gaussian fixed point $\lambda^* = 0, (v_\Delta/(v_F k_F))^* = 0$ with stable flow lines toward it. This suggests second order quantum phase transition between Ising nematic ordered and disordered phases, in the presence of half-Dirac fermions in the background superconducting state. Interpreting the fermion-Ising nematic boson interaction as a decay process of nematic Ising order parameter scalar field into half-Dirac nodal fermions, we find that the theory behaves as systems with dynamical critical exponent $z = 1$. The nematic critical fluctuations lead to broadening of quasiparticle spectral function except at the region near the half-Dirac nodes where 'Fermi arc-like' sharp peak of spectral weight appears. The nematic critical fluctuations do not modify much the anisotropy of such peak. We however found critical point λ_c, directly related to that of ϕ field transition, around which the Fermi arc of spectral function collapses.

I. INTRODUCTION

Quantum phase transition in strongly correlated systems such as high T_c superconductors is one of the most active topics in condensed matter physics. In cuprates and the recently discovered iron-based family of high T_c superconductors, there exists a quantum critical point at $T = 0$ deep inside the superconducting dome that represents such quantum phase transition(Fig. 1a),b)). This QCP also separates tetragonal and orthorhombic crystal structures and thus represents structural phase transition at zero temperature. It has been argued that the orthorhombic state is described by the so-called Ising nematic order [1,7,8] and such structural transition in cuprates[2,3] and iron-based superconductors[4,5,6] (where d-wave symmetry was assumed) is nematic transition. The general phase diagram of iron-based superconductors illustrated in Fig. 1*b*) shows that there is a tetragonal to orthorhombic structural phase transition at some finite temperature in the undoped case down to $T = 0$ at a critical doping x_c deep inside the dome where the Ising nematic order coexists with the $s_\pm$-wave superconducting state. At $T = 0$ this critical doping is a quantum critical point between Ising ordered state and Ising disordered state. The theory of quantum phase transition at this quantum critical point is the focus of this work.

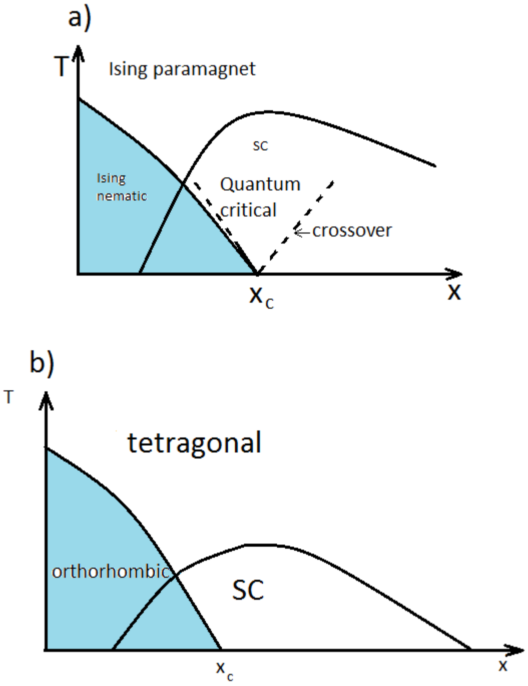

FIG.1 a)Quantum phase transition in cuprates with the quantum critical point and quantum critical region nearby. b) Typical phase diagram of iron-based superconductors with similar quantum critical point. In both a) and b), the parameter x is defined as and $x_c = -r$ and $x = -r(\lambda)$ as given in Eqs. (2) and (31). Physically, x may represent doping level, pressure, or other appropriate experimental quantities.

The quantum phase transition in cuprates that relates structural phase transition with nematic order was first studied using renormalization group approach[11, 12] which showed using perturbative RG calculation at fixed N_f with ϵ expansion around $3+1$ dimensions that the velocity anisotropy in the nodal fermion action and the anisotropic coupling between nodal fermion and Ising nematic order leads to a fluctuation-induced first order phase transition, as indicated by the runaway RG flows. A large-N_f study of the same system but in $2+1$ dimensions[2] however found a second order quantum phase transition and has finite renormalized velocity anisotropy as compared to Dirac-like theory such as QED_3 which found velocity anisotropy to be irrelevant. Another RG study on the same system in $2+1$ dimensions[3] found vanishing velocity anisotropy ratio $(\frac{v_\Delta}{v_F})^* = 0$ as the fixed point.

The coupling between nodal quasiparticles to the nematic order was argued to be the most effective driving force of the structural transition. The presence of nodes and the resulting nodal quasiparticles in d-wave cuprates is therefore of crucial importance here. On the other hand, from the aspect of gap symmetry, iron-based family was originally thought to have isotropic $s_\pm$ wave symmetry, thus ruling out the presence of nodes. However it was found later that the electron Fermi pocket in iron-based superconductors admits anisotropic gap and thus possible existence of nodes.

In a related development, it has been shown recently that iron-based superconductors can have the so-called accidental ('zero') node(Fig. 2)) at the electron pocket[9,10] due to the gap anisotropy where the gap just touches the Fermi surface, that is, it is right at the onset of being gapless. In the simplest model, we can represent it by $\Delta(\theta) = \Delta_0(1 - cos4\theta)$(Fig. 2). Such accidental zero has anisotropic dispersion which in linear in p_x direction and quadratic in p_y direction or vice versa. One can therefore interpret such zero as "half-Dirac" node, because it has Dirac spectrum in one direction but has parabolic dispersion in the perpendicular direction as that for free particle. This accidental node is robust and persists to zero temperature where we can have a quantum phase transition between fully gapped (nodeless), zero and nodal states by tuning appropriate parameters, e.g. the coupling constants in the Hamiltonian. Such gapless point is accidental because it does not arise from or protected by symmetry. This kind of nodes however has recently been shown to exist within *finite* regime of microscopic parameter space (the strength λ_h of the inter-electron pockets hybridization)[26] and so this makes it interesting to study the nature of quantum phase transition in iron-based superconductor compounds with such peculiar gapless point. This is the purpose of this work.

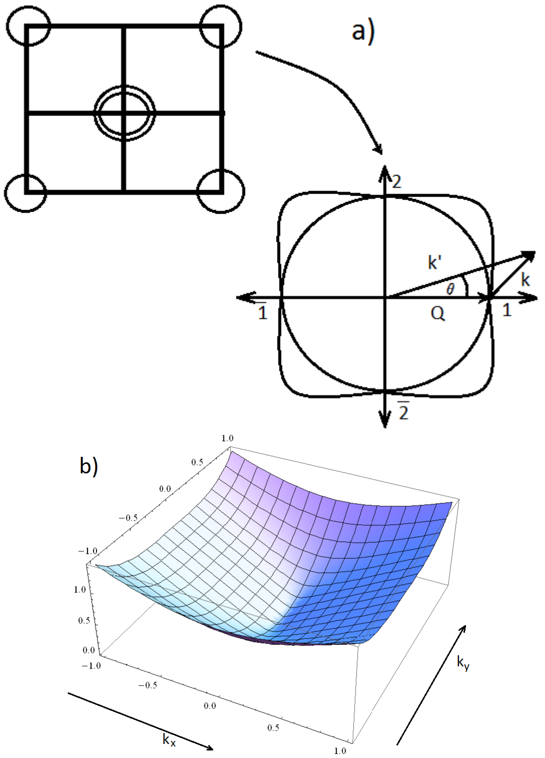

FIG. 2 a)Iron-based superconductors'(reduced) Brillouin zone and the electron Fermi surfaces ('pockets') at $(\pm\pi, \pm\pi)$ and hole pockets at $\Gamma = (0, 0)$. The electron pocket has anisotropic gap and its critical half-Dirac nodes paired as $1\bar{1}$ and $2\bar{2}$.b)The profile of a half-Dirac node. Energy $E \sim k_x$ in x direction but $E \sim k_y^2$ in y direction.

We summarize our *main results* as follows. First,the quantum phase transition in iron-based superconductors with half-Dirac node described by half-Dirac fermion-Ising nematic field theory has stable fixed point $\lambda^* = 0, (v_\Delta/(v_F k_F))^* = 0$ with no relevant interaction away from it in the $\lambda - v_\Delta/(v_F k_F)$ parameter space and no non-trivial interacting fixed point. Second, on the dynamical properties of the quantum phase transition characterized in terms of response function describing quasiparticle-nematic coupling, we find that the system response effectively has dynamical critical exponent $z = 1$. The nematic critical fluctuations lead to broadening of quasiparticle spectral function except in region near the node where we have 'Fermi arc'-like spectral ridge. Nematic fluctuations however do not affect much the degree of spectral peak anisotropy. However, the spectral ridge collapses in the vicinity of nematic QCP while it is well defined far away from QCP, both in ordered and disordered phases of nematic order. This signifies distinct quantum critical behavior from d-wave cuprates. This also emphasizes the distinction between the quantum critical $(T = 0)$ behavior of quasiparticle Fermi arc and its classical thermal phase transition counterpart, describable in terms of Kosterlitz-Thouless transition, with regards to the effect of order fluctuations(nematic Ising scalar order in the former and XY order in the latter).

We begin the formulation of the theory that give the above results in Section II by giving the low energy effective action for this problem, considering the large-N_f version and computing the needed field theoretical quantities to proceed with the RG. Then we analyze the structure of RG equations in Section III. We then discuss the nature of the quantum phase transition from response and spectral functions in Section IV. We end with discussion of the results and connection with other works on the problem.

II. LOW ENERGY EFFECTIVE FIELD THEORY OF SUPERCONDUCTING - ISING NEMATIC TRANSITION IN HALF-DIRAC NODAL IRON-BASED SUPERCONDUCTORS

To describe half-Dirac nodes, we can start with standard Bogoliubov-de Gennes Hamiltonian describing Cooper paired electrons and approximate the Hamiltonian around the nodes in momentum space[9]. We then construct the effective low energy field theory action for the superconducting state - Ising nematic order phase transition which consists of the action for half-Dirac nodal fermionic quasiparticles part, scalar Ising (nematic) order part and the fermionic quasiparticle-Ising order interaction part. The fermions describe fermionic quasiparticles $\Psi, \overline{\Psi}$ living in the vicinity of half-Dirac nodes in electron Fermi surface while the Ising nematic scalar field ϕ describes the degree of lattice distortion from tetragonal lattice where $\langle\phi\rangle = 0$ to orthorhombic lattice where $\langle\phi\rangle \neq 0$. The coupling between such nodal fermions with nematic order has been argued to be the most relevant coupling as the most effective process is where the nematic order field scatters the fermions around the nodes.

In the actual physical situation, we have four fermion species for each of the pairs of (half-Dirac) nodes ($1\overline{1}$ and $2\overline{2}$), where we have spin up and down quasiparticles at one node and another set of spin up and down electrons at the partner node. In the $\frac{1}{N_f}$ technique, we generalize the spin up and down species into N_f "flavors" of fermions. The phenomenological field theory for this problem is then described by the following action

$$S_\Psi = \int \frac{d^2k}{(2\pi)^2} T \sum_{\omega_m} \sum_{a=1}^{N_f} \overline{\Psi}_{1,a}(-i\omega_m\gamma_0 + v_f k_x \gamma_1 + \frac{8v_\Delta}{k_F} k_y^2 \gamma_2)\Psi_{1,a} + \overline{\Psi}_{2,a}(-i\omega_m\gamma_0 + v_f k_y \gamma_1 + \frac{8v_\Delta}{k_F} k_x^2 \gamma_2)\Psi_{2,a} \qquad (1)$$

$$S_\phi = \int d^2x d\tau (\frac{1}{2}(\nabla\phi)^2 + \frac{1}{2}c^2(\partial_\tau\phi)^2 + \frac{1}{2}r\phi^2 + \frac{u}{4!}\phi^4) \quad (2)$$

$$S_{\Psi\phi} = \lambda \int d^2x \int d\tau \phi \sum_{n=1,2,a=1}^{N_f} \overline{\Psi}_{n,a}\gamma_1\Psi_{n,a} \qquad (3)$$

where

$$\Psi_{n,a}(\mathbf{k},\omega_n) = (c_{n,a,+}(\mathbf{k},\omega_n), c^\dagger_{n,a,-}(-\mathbf{k},-\omega_n), c_{n,a,+}(\mathbf{k}+\mathbf{Q},\omega_n), c^\dagger_{n,a,-}(-\mathbf{k}-\mathbf{Q},-\omega_n))^T \qquad (4)$$

$$\overline{\Psi}_{n,a} = \Psi^\dagger_{n,a}\gamma_0$$

and

$$\gamma_0 = \tau_1 \bigotimes \tau_3, \gamma_1 = i\tau_2 \bigotimes \tau_0, \gamma_2 = \tau_1 \bigotimes i\tau_2 \qquad (5)$$

with index $n = 1, 2$ representing the $1\overline{1}, 2\overline{2}$ pairs of nodes while $a = 1, 2, 3, .., N_f$ is the fermion flavor index. The momenta $\mathbf{k}, \mathbf{Q} = k_F\widehat{x}, \mathbf{k'} = \mathbf{k} + \mathbf{Q}$ are as defined in Fig. 2. The τ's are the usual 2×2 Pauli matrices. The details to obtain the fermion action are given in Appendix A. It is necessary to emphasize that N_f flavors do not imply spin N_f quantum number. The 4×1 Nambu spinor defined in Eq. (4) contains the two $N_f = 2$ flavors from the two nodes in $1\overline{1}$ or $2\overline{2}$.

Note that even though nematic order is normally represented by symmetric traceless second rank tensor [1, 7] due to the fact that inverting the "director" vector that characterizes the nematic state should give equivalent system, we write the Ginzburg-Landau action (2) for this theory in terms of Ising field because the free, non-interacting (without fermions) nematic phase transition falls within the Ising universality class. The coupling to fermions will in general able to change the universality class of the phase transition.

A. Symmetry Consideration and Character of Nematic Order

Nematic order is basically a $\mathbf{Q} = 0$ order that we have implicitly assumed to couple to spin singlet fermion bilinear. It can be characterized in terms of particle-hole and particle-particle pairing correlators,

$$\langle c^{\dagger}_{\mathbf{k}'} c_{\mathbf{k}'} \rangle = A_{\mathbf{k}'},$$

$$\langle c_{\mathbf{k}'} c_{-\mathbf{k}'} \rangle = (\Delta^{s}_{0}(-(cosk'_x + cosk'_y) + (1 + cosk_F)) + B_{\mathbf{k}'})e^{i\varphi} \tag{6}$$

where we have represented our half-Dirac nodal anisotropic s-wave gap as $\Delta(k'_x, k'_y) = \Delta^{s}_{0}(-(cosk'_x + cosk'_y) + (1 + cosk_F))$. Here φ is the overall superconducting phase and we assume superconducting background through the entire order-disordered phases of the nematic order parameter. An ideal electron Fermi surface of iron-based superconductors with square lattice, without any symmetry breaking interactions, has C_4(or C_{4v}, which has extra symmetry of reflection with respect to vertical planes passing the central axis) symmetry. Note that both charge neutral(ones that do not depend on the sign of the gap) and charged (ones that do) observables have this symmetry group, unlike in d-wave superconductors where only charge neutral observables have C_{4v} whereas charged ones have only C_{2v}. This symmetry group has four $1d$ irreducible representations (s-wave with basis function $f(k') = 1$, $d_{x^2-y^2}$ $(cosk'_x - cosk'_y)$, d_{xy} $(sink'_x sink'_y)$, and g $(sink'_x sink'_y(cosk'_x - cosk'_y))$ and one $2d$ irreducible representations $p(sink'_x, sink'_y)$[11]. With such pairing gap, it is clear that $A_{\mathbf{k}'} = 0, B_{\mathbf{k}'} = \phi$ (where ϕ is real field) breaks C_{4v} symmetry to C_{2v}. This is nematic order. So, symmetry arguments that characterize how nematic order couples to our half-Dirac nodal superconducting state suggest that nematic order parameter has s-wave symmetry where time-reversal symmetry is unbroken but the point group symmetry is reduced from C_{4v} to C_{2v} with basis function simply a unity function. The nematic order can be polarized along x or y direction. This extra s-wave component ϕ however will eliminate the half-Dirac nodes for $\phi > 0$ or change each of the half-Dirac nodes to two full Dirac nodes for $\phi < 0$. We can however have order parameter which breaks C_{4v} to C_{2v} while keeping the half-Dirac nodes intact which clearly must be higher order modes. From the 5 irreducible representations of C_{4v} point group symmetry, d_{xy} wave with basis function $sink'_x sink'_y$ can deliver such half-Dirac node-preserving C_{4v}-to-C_{2v} symmetry breaking order parameter. To be precise, we can add on top of our anisotropic gap $\Delta(k'_x, k'_y) = \Delta^{s}_{0}(1 + cosk_F - (cosk'_x + cosk'_y))$ an order parameter $B_{\mathbf{k}'} = \phi sin(k'_x - k_c) sin(k'_y - k_c)$ where $0 \leq k_c \leq k_F/\sqrt{2}$. The resulting gap for $\phi < 0$ is shown in Fig. 3 while for $\phi > 0$ the gap is Fig. 3 rotated by $\frac{\pi}{2}$.

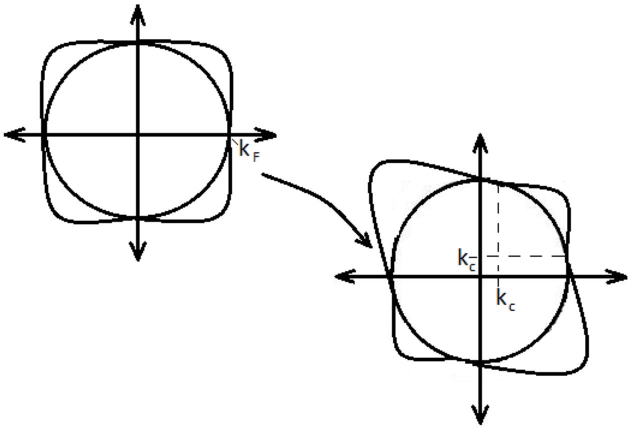

FIG. 3 C_{4v} to C_{2v} symmetric breaking of electron Fermi pocket gap with half-Dirac nodes.

The structural tetragonal to orthorhombic phase transition can easily be seen by rotating the gap function by $\frac{\pi}{4}$ to align with the lattice x and y axes.

The order parameter fluctuations when coupled to fermions will be relevant only when the wave vector $\mathbf{Q}$ carried by the order parameter is also the wave vector $\mathbf{Q}$ that connects the two nodes between which the fermions are scattered, by momentum conservation[11]. That is, the order parameter will scatter the fermions effectively and efficiently only when the momentum it carries is transferred entirely to the fermions. Otherwise the scattering is a virtual process which merely renormalizes the coupling constant without making a fundamental change in low energy theory. In this case, nematic order corresponds to $\mathbf{Q} = 0$ which means our theory consider scattering of fermions living in the vicinity of the same half-Dirac node by the nematic order fluctuations. Scattering by $\mathbf{Q} = (2k_F, 0)$ or $\mathbf{Q} = (0, 2k_F)$ should be described by some type of density wave but if we want to couple this density wave with fermions, the theory should describe coexisting superconducting and density wave phases. Experimentally as shown in Fig. 3 of Ref. 16, the superconducting phase does not coexist with the density wave phase but they do border each other, even though the Ising nematic order, where we have orthorhombic crystal structure, penetrates deep inside the superconducting regime, as illustrated earlier in Fig. 1b). We therefore essentially consider Ising-nematic quantum phase transition within the background superconductivity.

B. The Effective Action of Ising Nematic Order Parameter

In the large-N_f expansion, with the physical case $N_f = 2$ corresponds to spins up and down, we generalize the two spin polarizations of $S = \frac{1}{2}$ fermions into N_f "flavors" of fermions. We compute the effective action for bosonic nematic order parameter field $S_{eff}[\phi]$ by formally integrating out the fermion $\psi, \overline{\psi}$ from the original full action $S[\psi, \phi]$. This will give rise to nonlocal logarithmic term containing the fermion-nematic order field coupling constant λ and can thus be expanded perturbatively in powers of λ.

$$S_{eff}[\phi] = S_\phi - N_f \sum_{n=1,2} In(Det[-i\omega_m\gamma_0 + \overrightarrow{v}^n_F.\mathbf{k}\gamma_1 + \frac{8}{v_\Delta k_F}(\overrightarrow{v}^n_\Delta.\mathbf{k})^2\gamma_2 + \lambda\phi\gamma_1]) \quad (7)$$

Rescaling $\phi \to \frac{\phi}{\lambda}$ and $r \to rN_f\lambda^2$ and retaining the surviving terms, we have

$$S_{eff}[\phi] = N_f S^1_{eff}$$

where

$$S^1_{eff} = \int d^3x \frac{1}{2} r\phi^2 - \sum_{n=1,2} In(Det[-i\omega_m\gamma_0 + \overrightarrow{v}^n_F.\mathbf{k}\gamma_1 + \frac{8}{v_\Delta k_F}(\overrightarrow{v}^n_\Delta.\mathbf{k})^2\gamma_2 + \phi\gamma_1]) \quad (8)$$

where the $(\partial_\tau\phi)^2, (\nabla\phi)^2, u\phi^4$ terms vanish as we take the $N_f \to \infty$ limit. We will only consider the quadratic correction terms in ϕ while assuming that the renormalized quartic terms will remain sufficient to stabilize the effective Ginzburg-Landau type effective theory for ϕ without explicitly considering its renormalization. The effective action to quadratic order for ϕ can be written as

$$S^1_{eff}[\phi] = \int \frac{d^3k}{(2\pi)^3}(r + \Gamma_2(k))|\phi(k)|^2 \quad (9)$$

where

$$\Gamma_2(k) = \Pi_2(k_x, k_y, \omega) + \Pi_2(k_y, k_x, \omega) \quad (10)$$

The polarization function $\Pi_2(k_x, k_y, \omega)$ is given by the Feynman diagram in Fig. 4

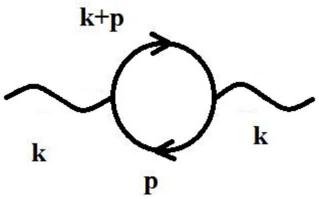

FIG. 4 The Feynman diagram for polarization function which contributes correction to quadratic part of ϕ effective action.

Using the representation (4) for Dirac γ matrices, the expression for the polarization function which is the correction to the boson propagator due to fermion is given by

$$\Pi_2(k_x, k_y, \omega) = \int \frac{d^3p}{(2\pi)^3} Tr[\gamma_1 G_\Psi(p)\gamma_1 G_\Psi(p+k)] \quad (11)$$

with

$$G^{-1}(p) = -i\omega\gamma_0 + v_f p_x\gamma_1 + \frac{8v_\Delta}{k_F}p_y^2\gamma_2 \quad (12)$$

where $\xi = \frac{8v_\Delta}{k_F}$ and we have focus only on node 1 as example. Despite its lengthy form, this polarization function is still even under time reversal of external momenta $(k_x, k_y, \omega) \to (-k_x, -k_y, -\omega)$ which can be verified by direct inspection. Also, by power counting, this expression must have dimension one in external momenta $[\Pi_2(k)] = k^1$ but is an even function of $k = (k_x, k_y, \omega)$.

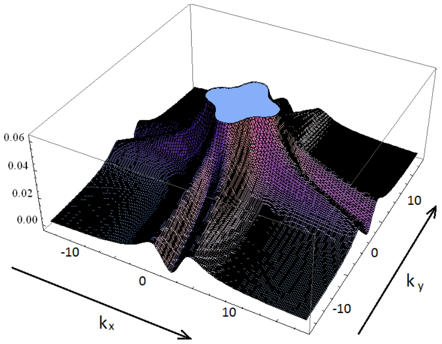

FIG. 5 The profile of polarization function $\Pi_2(k_x, k_y, \omega = -0.001\Delta\omega)$ computed numerically with $v_F = v_\Delta = 0.067eV\frac{a}{\pi}$ where $a = 0.1$ is the lattice spacing, with one unit of length $= 100A^o$. One unit of momentum $\Delta k = \frac{2\pi}{10a}$ and frequency $\Delta\omega = 0.271meV$. Here we chop off the tip to show the symmetry of the profile. The function has even parity in $(\mathbf{k}, \omega)$ and C_4 symmetry.

We compute numerically the value of $\Pi_2(k)$ in Eq.(8) as function of the two external momenta at a fixed external frequency and the result is shown in Fig. 5, which gives us some rough idea of how this quantity varies as function of momenta. The most important observation from Fig. 5 is that the polarization function profile has C_4 symmetry and that it is peaked around $\mathbf{k'} = (0,0)$ with respect to the center of electron pocket.

We also compute the $\frac{1}{N_f}$ fermion self-energy and vertex corrections to nematic scalar field action needed for the following sections, the details of which are given in Appendix B. Regarding the nature of quantum phase transition, we will show that the quantum phase transition between Ising nematic ordered and disordered phases, in the presence of half-Dirac fermions in the background superconducting state, is second order phase transition with the non-interacting fixed point of Dirac fermions.

III. RENORMALIZATION GROUP EQUATIONS STRUCTURE OF THE THEORY

One thing that can be noticed from fermion action (1) is that the momentum is linear in k_x but quadratic in k_y. If we want this action to be invariant under rescaling of momenta and frequency, the scaling dimension for k_x must be twice of that of k_x. But here for the purpose of RG calculations we choose to use the same scaling dimension for k_x and k_y. Further, rather than using a dynamical critical exponent z for the scaling of frequency, we use the same scaling dimension for ω as that for k_x and k_y. The reason is RG will naturally fix the scaling dimension for ω implicitly inside the coefficients of RG equations. Therefore, we write the scaling of momenta, frequency as follows;

$$k_x = k'_x e^{-l}$$

$$k_y = k'_y e^{-l}$$

$$\omega = \omega' e^{-l} \tag{13}$$

The scaling of bosonic and fermionic scalar fields is obtained by considering renormalization of the time derivative term in S_ϕ and S_ψ respectively which gives scaling dimensions $dim[\Phi(k)] = -\frac{5}{2}$ and $dim[\Psi(k)] = -2$. This implies field scaling of the form

$$\Phi(k_x, k_y, \omega) = \Phi'(k_x, k_y, \omega) e^{-\int_0^l dl'(\frac{5}{2} - \frac{\eta_b}{2})}$$

$$\Psi(k_x, k_y, \omega) = \Psi'(k_x, k_y, \omega) e^{-\int_0^l dl'(2 - \frac{\eta_f}{2})} \tag{14}$$

By similar simple power counting at tree level, where interaction is assumed to be nonsingular, as is the case here with Yukawa type of coupling, it can be easily checked that the scaling dimension of Yukawa coupling constant is $dim[\lambda] = \frac{1}{2}$ which shows that the coupling to nematic order parameter is a relevant perturbation to the $(\frac{v_\Delta}{k_F v_F})^* = 0$ fixed point associated with the half-Dirac nodal quasiparticles of the iron-based superconductors. The mass r term on the other hand has scaling dimension $dim[r] = \frac{1}{\nu} = 2$ at tree level which shows it is also relevant parameter and must thus be evaluated in the RG analysis, the RG flow equation of which can in general be written as

$$\frac{dr}{dl} = \frac{1}{\nu} r = (2 - \eta_b) r \tag{15}$$

where the generally nonvanishing anomalous dimension η_b of bosonic scalar field ϕ enters. As a comparison, one may prefer to use a rescaling of momenta and frequency that leaves the fermion action invariant,

$$k_x = k'_x e^{-l}$$

$$k_y = k'_y e^{-\frac{l}{2}}$$

$$\omega = \omega' e^{-l} \tag{16}$$

Again considering renormalization of the time derivative term in S_ϕ and S_ψ respectively gives scaling dimensions $dim[\Phi(k)] = -\frac{9}{4}$ and $dim[\Psi(k)] = -\frac{7}{4}$. This implies field scaling of the form

$$\Phi(k) = \Phi'(k) e^{-\int_0^l dl'(\frac{9}{4} - \frac{\eta_b}{2})}$$

$$\Psi(k) = \Psi'(k) e^{-\int_0^l dl'(\frac{7}{4} - \frac{\eta_f}{2})} \tag{17}$$

We still arrive at the same conclusion that the Yukawa coupling is relevant perturbation away from the $(\frac{v_\Delta}{k_F v_F})^* = 0$ fixed point with scaling dimension of $dim[\lambda] = \frac{3}{4}$.

We investigate the structure of the RG equations by starting from the logarithm of cut-off derivative of fermion self energy and vertex functions rather than using the usual momentum shell transformation. The RG equation should be of the form given by

$$\Lambda \frac{d\Sigma}{d\Lambda} = (C_0^0 \gamma_0 + C_1^0 \gamma_1)\omega + (C_0^1 \gamma_0 + C_1^1 \gamma_1) k_x + C_2(k_y) \tag{18}$$

$$\Lambda \frac{d\Xi}{d\Lambda} = C_3 \gamma_1 \tag{19}$$

The k_y part is written to indicate that it has some unknown nonlinear dependence on k_y, unlike the k_x and ω

parts. We also note that the inverse propagator is not homogeneous function of ω, k_x and k_y anymore and this has tremendous effect on the complexity of the analysis. Before proceeding further, we first find the relations between the C's coefficients and the anomalous dimensions η_f and η_b. One caveat before doing this is that the RG equations (14) and (15) are 4×4 matrix equations rather than scalar equations. The relation involving η_f is obtained by fixing the kinetic time derivative part in S_ψ while that for η_b is obtained by fixing the Yukawa coupling term. The latter is done because the nematic order action S_ϕ does not have kinetic term upon integrating out the fermions, as can be seen in Eq. (6) which has a non-local term given by the logarithmic part. This non-local term will overpower the local terms of S_ϕ except the $r\phi^2$ term. This can be seen by considering the scaling dimensions of each of the terms in S_ϕ. Earlier we obtained $dim[\Phi(k)] = -\frac{5}{2}$ or $dim[\phi(x,y,t)] = \frac{5}{2}$ and this implies $dim[r] = 2$ and $dim[u] = 1$. We see that the quartic coupling u is less relevant than the quadratic coupling r and so the former can be omitted. The derivative terms on the other hand will also have diminishing effect because they are marginal terms. We are therefore allowed to retain only the $r\phi^2$ and omit the other terms in S_ϕ.

To find the relations between the C's coefficients and the anomalous dimensions η_f and η_b, fixing the kinetic time derivative part in S_Ψ, we have

$$\eta_f = \gamma_0^{-1} C_0^0 \gamma_0 + C_1^0 \gamma_1 = \begin{pmatrix} C_1^1 - C_1^0 & 0 & 1 & 0 \\ 0 & C_1^1 + C_1^0 & 0 & 0 \\ 0 & 0 & C_1^1 + C_1^0 & 0 \\ 0 & 0 & 0 & C_1^1 - C_1^0 \end{pmatrix} \tag{20}$$

which demonstrates a "pair-wise" pattern associating fermions living at the same nodes (fermions 1 and 4 at node 1 (or 2) and fermions 2 and 3 at node $\bar{1}$(or $\bar{2}$). We will also see this pattern later in the structure of RG flow equations for v_F and v_Δ which has crucial significance as hinted in the abstract. If we argue that the anomalous dimension η_f is a universal characteristic of fermion which should be independent of the where the fermion lives in momentum space, then we have to conclude

$$C_0^0 - C_1^0 = C_0^0 + C_1^0 = \eta_f$$

and therefore

$$C_0^0 = \eta_f, C_1^0 = 0 \tag{21}$$

Following similar procedure to η_b by fixing the Yukawa coupling, we have

$$\eta_b = 1 + 2C_3 - 2\eta_f \tag{22}$$

Here, $C, \eta_f \ll 1$ but $\eta_b \sim 1$.

The observation that we only have one equation for boson field anomalous dimension fits perfectly with the fact that we only have one real scalar boson field. We derive these RG equations for coefficients C's by evaluating directly $\Lambda \frac{d\Sigma}{d\Lambda}$ from the expression for the self energy $\Sigma(k,\omega)$. Unfortunately, since the propagator is not homogeneous function of momenta and frequency, the resulting equations will depend explicitly on the cut-off momentum Λ. We can use hard cut-off since this is the simplest possible cut-off function and hope this choice will minimize the cut-off dependence of the final results. Computation of C's as functions of v_F and v_Δ can only be done numerically. Rather than pursuing the detailed numerical evaluation of the flow, we instead analyze the structure of RG flow equations of the theory and make qualitative but yet definitive conclusions about the critical properties of the system.

The RG equations for Fermi and gap velocities are derived by considering the renormalization of terms that contain these velocities in the fermion action S_Ψ. Fixing the $v_F k_x$ term, we have

$$\frac{dv_F}{dl} = (-\eta_f - C_0^1 \gamma_1^{-1} \gamma_0 + C_1^1) v_F \tag{23}$$

where $v_F = (v_{F1}, v_{F2}, v_{F3}, v_{F4})^T$.
whereas from renormalization of $\frac{8 v_\Delta p_y^2}{k_F}$ term we have

$$\frac{dv_\Delta}{dl} = (-\eta_f - (C^2 \gamma_2^{-1} \gamma_0 + C^2 \gamma_2^{-1} \gamma_1)) v_\Delta \tag{24}$$

where $v_\Delta = (v_{\Delta 1}, v_{\Delta 2}, v_{\Delta 3}, v_{\Delta 4})^T$. We only consider the leading linear order terms for the RG equations here. Using the γ matrices as defined in (4), we have

$$\begin{pmatrix} \frac{dv_{F1}}{dl} \\ \frac{dv_{F2}}{dl} \\ \frac{dv_{F3}}{dl} \\ \frac{dv_{F4}}{dl} \end{pmatrix} = \begin{pmatrix} M_\alpha & 0 & 1 & 0 \\ 0 & M_\beta & 0 & 0 \\ 0 & 0 & M_\beta & 0 \\ 0 & 0 & 0 & M_\alpha \end{pmatrix} \begin{pmatrix} v_{F1} \\ v_{F2} \\ v_{F3} \\ v_{F4} \end{pmatrix} \tag{25}$$

where

$$M_\alpha = -\eta_f - C_1^1 + C_1^0, M_\beta = -\eta_f - C_1^1 - C_1^0$$

$$\begin{pmatrix} \frac{dv_{\Delta 1}}{dl} \\ \frac{dv_{\Delta 2}}{dl} \\ \frac{dv_{\Delta 3}}{dl} \\ \frac{dv_{\Delta 4}}{dl} \end{pmatrix} = \begin{pmatrix} -\eta_f & -2C^2 & 0 & 0 \\ 0 & -\eta_f & 0 & 0 \\ 0 & 0 & -\eta_f & 0 \\ 0 & 0 & -2C^2 & -\eta_f \end{pmatrix} \begin{pmatrix} v_{\Delta 1} \\ v_{\Delta 2} \\ v_{\Delta 3} \\ v_{\Delta 4} \end{pmatrix} \tag{26}$$

We have RG flow equations for v_F and v_Δ involving coefficients C's that are themselves functions of v_F and v_Δ. We can see here that each of the four fermion components of the 4×1 Nambu spinor has its own RG equations for v_F and v_Δ. This means that in general v_F and v_Δ will flow differently between these four fermion components under RG. This feature arises purely from the symmetry property of anisotropic gap of electron pocket which is clearly different from d-wave cuprates case where one RG equation for v_F and another RG equation for v_Δ are sufficient. If we consider the hypothesized fixed point $(\frac{v_\Delta}{v_F k_F})^* = 0$, which necessarily requires $(v_\Delta)^* = 0$ but $(v_F)^* \neq 0$, from $\frac{dv_F}{dl} = 0$ we will have $C_0^1 = 0$ and $C_1^1 = -\eta_f$ at the fixed point which set the final condition for the RG flow equation for the coefficients C_0^1 as $C_0^1(v_\Delta^* = 0, v_F^* \neq 0) = 0$ and C_1^1 as $C_1^1(v_\Delta^* = 0, v_F^* \neq 0) = -\eta_f$. This fixes the final condition for both coefficients in the RG flow for v_F. Considering the $\frac{dv_\Delta}{dl} = 0$ at fixed point, we obtain no new information but the confirmation that the RG flow equation $\frac{dv_\Delta}{dl}$ is consistent at the fixed point. This consistency at least offers some posteriori justification of our fixed point assumption.

If we denote the four fermions constituting the 4×1 Nambu spinor Eq. (4) by A, B, C and D respectively, as depicted in Fig. 2 so that $\overline{\Psi}_{n,a} = (A, B, C, D)^T$, looking at the structure of the flow equations given in equations (22) and (23), we can see that the flow equations for fermion A have equivalent structure to those of fermion D while those of fermion B are equivalent in structure to those of fermion C. This means that the RG flow associated with the spin up nodal fermion at $(k_F, 0)$ is the same as that of spin down nodal fermion at $(k_F, 0)$. Likewise, the RG flow of the spin up nodal fermion at $(-k_F, 0)$ is identical to that of spin down nodal fermion at $(-k_F, 0)$. This agrees with the expectation that the Fermi velocity of two fermions living at the same half-Dirac node must flow identically but this also shows a new important observation that the Fermi velocity at the two half-Dirac nodes can in general flow differently under RG. One direct physical implication of Fermi velocity flowing to different values between fermions at different nodes is that, since $\epsilon_k = v_F k_x + O(k^2)$ and $v_\Delta = \nabla_k \Delta(k)|_{\mathbf{k}=(k_F,0)} = \frac{\Delta_0}{k_F}$, the originally C_4 symmetric electron pocket gap is deformed under RG flows(where nematic order comes into play implicitly via its coupling to nodal Fermions) and thus the C_4 is broken(Fig. 3)).

The relevance of nematic-quasiparticle Yukawa coupling at tree level led to the suggestion of the existence of a non-trivial fixed point $\lambda^* \neq 0$ along the coupling λ axis[2]. This fixed point thus has $(\frac{v_\Delta}{v_F})^* = 0$ along the other axis. We have shown earlier that with half-Dirac spectrum, nematic order is still relevant coupling despite with slightly different scaling dimension. Therefore at tree level one would naively expect that λ will flow away from the noninteracting Gaussian fixed point $\lambda^* = 0$. However, if we consider one loop diagrams for renormalization within minimal subtraction scheme and dimensional regularization, simple power counting shows that the all the diagrams have no divergence. This shows that the Yukawa coupling has vanishing β function and is thus irrelevant coupling at one loop level, despite being relevant at tree level.

One of the signatures of the proposed Ising nematic phase is its effect on the superconductor quasiparticle spectral function. In particular,quantum critical nematic fluctuations are expected to damp the quasiparticle spectral function, resulting in significant change in the spectra. In d-wave superconductor, it was shown [2] that quantum critical nematic fluctuations overdamps the quasiparticles in direction normal to the Fermi surface while weakly damps them in direction tangential to the Fermi surface around the node, resulting in highly anisotropic spectral function in the form of very narrow wedge. We will show soon that in the case of iron-based superconductors with anisotropic gap in electron pocket the situation is rather different.

IV. THE NATURE OF THE QUANTUM PHASE TRANSITION FROM DYNAMICAL PROPERTY OF THE THEORY

In this section, we will investigate the nature of this quantum phase transition [18,19,20] from the system's critical dynamics. The interaction between half-Dirac nodal quasiparticle and nematic Ising order field can be interpreted as some kind of "damping" process where Ising order parameter ϕ decays into half-Dirac nodal quasiparticles Ψ. One can then write a phenomenological field theory characterized by a dynamical critical exponent z that measures the degree of the damping of the half-Dirac nodal quasiparticles by the nematic order parameter fluctuations. To quantify this dynamical process, we consider the finite temperature version of polarization function $\Gamma_2(\mathbf{k}, \omega_n)$ to Ising nematic scalar ordering field action due to half-Dirac nodal fermions (8). Since polarization function can also be interpreted as susceptibility $\chi_0(k, \omega_n)$ describing the system response, we can also use it to understand the nature of quantum critical phenomena[27,28] from this dynamical property around the quantum critical point at optimal doping level $x = x_c$, assuming that the half-Dirac node is intact by control of appropriate parameters. The susceptibility function $\chi_0(k, \omega_n)$ applicable to the finite temperature crossover around QCP is given by

$$\chi_0(k,\omega_n) = T\sum_{\omega_n}\int \frac{d^2p}{(2\pi)^2} Tr[\gamma_1 G(p,\Omega_n)\gamma_1 G(p+k,\Omega_n+\omega_n)] \tag{27}$$

where according to Eq. (8) we have to include the contribution of both pairs $1\overline{1}$ and $2\overline{2}$ of nodes. We are not particularly interested in the explicit form of the above expression but rather, in its form upon lowest order expansion in powers of k_x, k_y and ω_n where k_x, k_y are measured from the node as shown in Fig. 2. It can be shown that

$$\chi_0(k_x,k_y,\omega_n) = \chi_0(0,0,0) + a\omega_n^2 + b(k_x^2+k_y^2) + ... \tag{28}$$

which shows the presence of kinetic term ω_n^2 versus k_x^2, k_y^2 and thus implies dynamical critical exponent $z = 1$. We can contrast this with the Fermi liquid-spin density wave transition[18] for example which has low energy susceptibility of the form $\chi_0(k,\omega_n) = \chi_0(0,0) - c_1|\omega_n| - c_2k^2 + ...$ where the $|\omega_n|$ indicates the damping of order parameter fluctuations due to due to the coupling to nodal fermions at the nodes connected by the spin density wave ordering wavevector. Note that we obtain the above result Eq. (34) even without taking the asymptotic limit $v_\Delta \to 0$ or making a priori assumption that we have fixed point at $(v_\Delta/(v_F k_F))^* = 0$. This therefore independently agrees with our result that the field theory Eqs. (2,3,4) has fixed point at $(\frac{v_\Delta}{k_F v_F})^* = 0$ because then the fermions behave like those described by action $\sim \overline{\Psi}_{1,a}(-i\omega_m\tau^z + v_F k_x\tau^t)\Psi_{1,a} + \overline{\Psi}_{2,a}(-i\omega_m\tau^z + v_F k_y\tau^t)\Psi_{2,a}$ asymptotically in the limit $v_\Delta \to 0$ which has $z = 1$(In calculations involving fermion internal momenta we cannot take $v_\Delta = 0$ though).

We observe here that despite having Lorentz-symmetry breaking anisotropic dispersion, in the low energy limit our Ising nematic field theory behaves as undamped system characterized by $z = 1$. This suggests the Ising nematic field fluctuations are effectively undamped by its coupling to half-Dirac nodal fermions. This is only possible if (or rather, this implies that), at nemating quantum critical point, the quasiparticle density of states is very low or actually vanishes. We will shortly show more quantitatively that this is indeed the case, by directly computing the quasiparticle spectral function. Nematic critical fluctuations however do not necessarily change much the degree of anisotropy of quasiparticle spectrum, but rather, the quasiparticle *spectral weight* itself. This is to be compared with the result for the d-wave case [2] which found a very strong damping of nematic order parameter by quasiparticle excitations in such a way that the spectral function of the quasiparticle is significantly broadened everywhere in BZ except at narrow 'wedges' around Dirac nodes where the spectral function acquires a very anisotropic Fermi arc shape, being very narrow in direction perpendicular to the Fermi surface and very long in direction tangential to it. In other words, nematic critical fluctuations strongly enhance the velocity anisotropy of the d-wave nodal fermions. This later conclusion is however, as pointed out by Pelissetto et al.[21], very dependent on the use of nematic scalar field and tree level power counting result which casts the Yukawa coupling between nematic order and nodal quasiparticle as relevant. Higher loops and field theorist renormalization calculation of scaling dimension of the coupling constant of composite spin density wave rather than Ising nematic to nodal quasiparticles puts the coupling as marginal rather than relevant.

We now compute the half-Dirac quasiparticle spectral function to see more quantitatively the effect of nematic critical fluctuations. The spectral function is given by

$$A(\mathbf{k},\omega) = -2sgn(\omega)Im[G_{ab}(\mathbf{k},\omega)] \tag{29}$$

where $G_{ab}(\mathbf{k},\omega)$ is the nonvanishing $(a,b)-th$ element of the renormalized single quasiparticle Green's function given by $G^{-1}(\mathbf{k},\omega) = G_0^{-1}(\mathbf{k},\omega) - \Sigma(\mathbf{k},\omega)$. We consider the 4×4 matrix version of our theory with G_0 given in Eq. (10) and the self energy $\Sigma(\mathbf{k},\omega)$ can be decomposed as $\Sigma(\mathbf{k},\omega) = \Sigma^a\gamma_0 + \Sigma^b\gamma_1 + \Sigma^c\gamma_2$, the details of which are given in Appendix C. We compute the polarization function numerically and hence the self energy as well and input the result to the following expression for the spectral function,

$$A(\mathbf{k},\omega) = 2sgn(\omega)\frac{\omega + Im(\Sigma^a(\mathbf{k},\omega))}{(Im(\Sigma^a(\mathbf{k},\omega))+\omega)^2 + (\Sigma^b(\mathbf{k},\omega) - v_F k_x)^2 + (\Sigma^c(\mathbf{k},\omega) - \frac{8v_\Delta}{k_F}k_y^2)^2} \tag{30}$$

We present here the dependence of quasiparticle spectral function on velocity ratio v_Δ/v_F shown in Fig. 6.

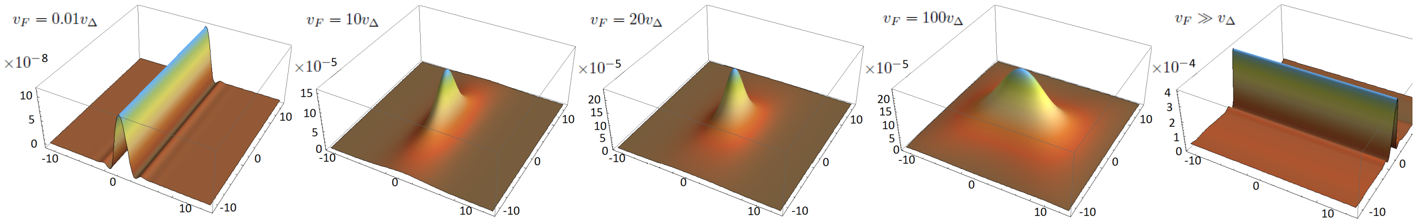

FIG. 6 The quasiparticle spectral function $A(\mathbf{k}, \omega = -0.001\Delta\omega)$ centered at the node $\mathbf{k'} = (k_F, 0)$ with respect to the center of electron pocket, as function of anisotropy v_F/v_Δ. We use as parameter values; one unit of momentum $\Delta k = \frac{2\pi}{10a}$, the lattice spacing $a = 0.1$, with one unit of length $= 100A^o$ and frequency $\Delta\omega = 0.271meV$ and at $v_F/v_\Delta = 1$, we use $v_F = v_\Delta = 0.067eV\frac{a}{\pi}$.

We note that in the limit of $v_F \gg v_\Delta$, we have extremely anisotropic spectral weight along one of the two (e.g. x) orthogonal axes. As the ratio between the two velocities is tuned to order of unity, the anisotropy decreases but we still have relatively anisotropic spectral function. At $v_F \approx v_\Delta$ the spectral peak is actually still very anisotropic with 'Fermi arc'-like shape rather than round one. It takes some large ratio $v_F/v_\Delta > 1$ in order to achieve a roughly round spectral peak. At the other limit of the anisotropy where $v_\Delta \gg v_F$, we have extremely anisotropic ridge perpendicular to the ridge in the opposite limit. This behavior clearly derives from the non-Lorentz symmetric form of fermion action.

The extent of the effect of nematic critical fluctuations on quasiparticles is best investigated by considering the dependence of spectral function on the strength of quasiparticle-nematic Yukawa coupling λ. We expect that, in terms of anisotropy, the coupling to nematic order does not change much the anisotropy of the quasiparticle spectral function. The effect of nematic order is however more towards the magnitude of spectral peak and we expect that there could be nontrivial change in the profile of spectral function near some critical value $\lambda = \lambda_c$ with regard to the presence or absence of Fermi arc. This can readily be expected from the fact that the effective action $S^1_{eff}[\phi]$ in Eq. (8) can eventually be written as,

$$S^1_{eff}[\phi] = \int \frac{d^3k}{(2\pi)^3}(r - r(\lambda))|\phi(k)|^2 + ...$$

$$= \int \frac{d^3k}{(2\pi)^3}(\lambda_c^2 - \lambda^2)|\phi(k)|^2 + ... \tag{31}$$

where the mass parameter $r \sim \lambda_c^2$ corresponds to the critical coupling while $r(\lambda) \sim \lambda^2$ comes from the the Yukawa nematic-quasiparticle coupling. Intuitively speaking, for $\lambda \ll \lambda_c$(deep inside disordered state of ϕ), we have $\langle\phi\rangle = 0$ and so that in computing the renormalized fermionic quasiparticle propagator we can simply substitute $\langle\phi\rangle = 0$ for ϕ. Likewise, for $\lambda \gg \lambda_c$(deep inside ordered state), we have $\langle\phi\rangle \neq 0$ and we can simply substitute this $\langle\phi\rangle$ for ϕ. In both cases, the quasiparticle spectral ridge is well defined. Things are less clear in intermediate region near λ_c as to what happens to the spectral peak. To investigate the physics in this regime and also to verify the simple intuitive picture in deep ordered and disordered phases, we again compute numerically the spectral function but this time we vary the Yukawa nematic-fermion coupling strength λ. We find that spectral function has sharp ridge in the ϕ-disordered state ($\lambda < \lambda_c$) and much heavily broadened spectral peak in ϕ ordered state (corresponding to massive fermions) but the spectral peak collapses in the intermediate region, which directly corresponds to critical point λ_c in $S^1_{eff}[\phi]$. This can actually be checked analytically. From Eqs. (37) and (C2) in Appendix C, it is clear that $A(\mathbf{k}, \omega)$ vanishes at a critical value λ_c, which in the limit of $r \gg \lambda^2$, is approximately given by

$$\lambda_c^2 = \frac{r|\omega|}{\int \frac{d^3p}{(2\pi)^3}\frac{(\omega+\Omega)}{[(\omega+\Omega)^2+v_F^2p_x^2+\eta^2p_y^4]}} \tag{32}$$

with $\eta = \frac{8v_\Delta}{k_F}$ and we have focused on the nodal point ($k_x = k_y = 0$) at which the peak is centered. This result clearly quantitatively confirms our earlier intuitive prediction. This $T = 0$ critical point shows different behavior with regard to spectral peak than what occurs in thermal phase transition in cuprates where Fermi arc emerges as the temperature (here the Yukawa coupling λ acts as temperature with $\lambda_c - \lambda \sim T - T_{KT}$) is increased above T_{KT} in a Kosterlitz-Thouless type of transition when analyzed with XY model[29]. In the QPT described by Eq. (37), in both deep ordered and disordered regions of ϕ field, the fermionic quasiparticles behave as free fermions (but being massive and massless respectively) and are well defined in these two. Only in the vicinity of QCP the nematic quantum fluctuations are able to disrupt the definition of quasiparticles. This underlines the difference of the physics of quantum and thermal phase transition in these high T_c superconductors and at the same time provide validity check to our theory.

V. DISCUSSION AND SUMMARY

We have emphasized the analysis of RG structure of the low energy effective theory of half-Dirac iron-based superconductors to deduce its nematic quantum critical properties. Simple power counting at tree level shows that nematic order is *relevant* perturbation away from the $(\frac{v_\Delta}{k_F v_F})^* = 0$ fixed point of the half-Dirac nodal quasiparticles. However, all one-loop diagrams in the context of dimensional regularization plus minimal subtraction scheme of field theorist renormalization have no divergence which suggests that at one loop level the nematic order is *irrelevant* coupling and the theory thus has non-interacting fixed point and that $(\frac{v_\Delta}{k_F v_F})$ is irrelevant parameter. The RG flow diagram therefore has stable flow lines both along the Yukawa coupling λ axis and as well as the $(\frac{v_\Delta}{k_F v_F})$ axis. The theory therefore does not have finite coupling fixed point which is the case for *d*-wave cuprate superconductor. The C_4 symmetry breaking leads to peculiar nature of relevance(or irrelevance)of the RG parameters around the electron pocket where v_F is found to be marginal coefficient while $\frac{v_\Delta}{k_F v_F}$ can be marginal or irrelevant depending on which of the two equally valid options of momenta-frequency rescaling scheme we choose. The $k_x \leftrightarrow k_y$ equivalence of C_4 symmetry is broken by this anisotropy and this suggests that the gap deformation instability associated with nematic order is the phenomenological physical picture of structural phase transition in half Dirac nodal iron-based superconductors. The whole analysis assumed that the half-Dirac nodes remain intact all along during RG flow. The possibility for this to be the real situation is strongly supported by recent work in Ref. 26 where it was shown the such kind of nodes is guaranteed to exist as long as the strength λ of hybridization between the two electron pockets (the interpocket hopping term with momentum (π, π, π)) is less than some critical value λ_c. Our theory is therefore valid within *finite* regime in parameter space rather than only at a critical point that can only be achieved by fine tuning.

In describing the physical mechanism of structural phase transition in high T_c superconductors, the nematic phase couples most relevantly to the quasiparticles while at the same time couples to lattice distortion which measures the degree of structur deformation. The nematic phase can be electronic (charge) or spin nematic phase and is still currently actively investigated experimentally[24]. The gap anisotropy in iron-based superconductors is believed to be determined by orbital content[25] of the electron Fermi pocket and this directly suggests connection of structural phase transition to orbital ordering as orbital ordering is driven by redistribution of occupation density of d_{xz} and d_{yz} orbitals in $(\pi, 0)$ and $(0, \pi)$ electron pockets(in extended Brillouin zone). We see therefore a self-consistency of picture of the physics of structural phase transition as related to the symmetry breaking of anisotropic gap on the electron pocket with the proposal of orbital ordering-driven structural phase transition. It was also shown that in orbital ordering picture [17] the structural phase transition is in the Ising universality class and can be described by effective Hamiltonian

$$H_{SPT} = -J_{SPT} \sum_{\langle i,j \rangle} M_i M_j \tag{33}$$

which is not inconsistent with our Ising nematic ordering picture and idea that nematic ordering can be related to orbital ordering.

Another important support for nematic-driven structural phase transition[22] is provided by the order of phase transition. In the 122-family, the structural and magnetic ordering phase transitions become a single first order phase transition while in 1111-family, they become two separate second order phase transitions. Eventually the idea of nematic phase offers very good explanation of this kind of behavior[23]. In magnetic ordering, the order parameter is characterized by vector while in nematic phase the order parameter is director, which is headless vector which we have represented with Ising nematic scalar field because the phase transition is in Ising universality class. While the magnetic ordering phase transition is second order, the nematic phase transition is known to be very weakly first order. This suggests that in 122 compound, the nematic ordering is very dominant and controls the magnetic ordering so that they become a single first order phase transition. In 1111 compound on the other hand, the nematic and magnetic orderings are equally strong and occur in sequence where the cubic term in the Ginzburg-Landau free energy description of nematic order diminishes and we thus obtain our effective field theory description Eq. (15) and second order phase transition for both ordering.

The very existence of nematic phase in high T_c superconductors including iron-based superconductors is actually still a very much debated issue. Several important fundamental questions include, if such phase does indeed exist, what kind of nematic phase it is precisely, electron nematic or spin nematic? It is then interesting to ask the differences in physical consequences of these two (or other) possible forms of nematic phase. Also, if indeed this phase exists, where does it exists in the phase diagram? In the paramagnetic tetragonal phase at $T \geq T_S$ or in the magnetically ordered phase $T \leq T_N$ or in between the two or instead it spreads over different regimes? Latest experiment [24] suggested the presence of an intrinsic spin nematic fluid even in the isotropic tetragonal phase $T \geq T_S$ of $BaFe_2As_2$ based on the observed anisotropy of spin wave excitations that persist well inside this region in the phase diagram. It is an open problem left for future work to construct a theory based on spin nematic fluid that can explain structural phase transition in iron-based superconductors.

ACKNOWLEDGMENTS

The author thanks Predrag Nikolic, Victor Vakaryuk, Adrian del Maestro, Yuan Wan, Collin Broholm, Eun-Ah Kim, Andrey V. Chubukov, Cenke Xu, Weicheng Lv, and Yejin Huh for helpful discussions. The author also thanks Kirill Melnikov, George Bruhn, and Jingsheng Li for their field theorist's insights on renormalization of non-Lorentz invariant field theory.

Appendix A: Details on the Fermion Action

We will give the details here the construction of fermionic quasiparticles action. We consider electron pocket with anisotropic gap associated with the fermionic quasiparticles, as illustrated in Fig. A1).

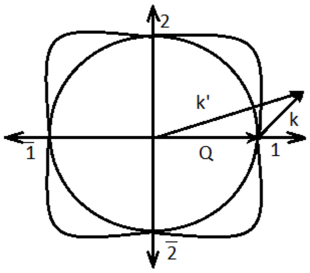

FIG. A1)Electron Fermi surface with critical half-Dirac node

The 'nesting' wave vector in this case is $Q = (\pm 2k_F, 0)$ or $Q = (0, \pm 2k_F)$, corresponding to 11 and 22 pairs of nodes respectively. The kinetic energy is measured relative to Fermi energy;$\zeta_{\mathbf{k}} = \varepsilon_{\mathbf{k}} - \varepsilon_F$ where $\mathbf{k} = \mathbf{K} + \mathbf{q}$ with $\mathbf{2K} = \mathbf{Q}$ as depicted in Fig.A1). Simple inspection on the geometry of the gap suggests that we have $\zeta_{\mathbf{k}} = -\zeta_{\mathbf{k}}$ and $\Delta(\mathbf{k} - Q_i) = \Delta(\mathbf{k}\ ) = \Delta(-\mathbf{k})$. We assume that the theory has standard BCS phenomenology with anisotropic s-wave symmetry at the electron Fermi surface with well defined, long-lived fermionic quasiparticles. We aim to write the fermion action as

$$S = \int \frac{d^2k}{(2\pi)^2} T \sum_{\omega_n} \sum_{n=1,2,a=1}^{N_f} \overline{\Psi}_{n,a}(\mathbf{k}, \omega_n) M \Psi_{n,a}(\mathbf{k}, \omega_n) \tag{A1}$$

where $\Psi(\mathbf{k}, \omega_n)$ is as given in Eq.(4). The general quasiparticle action at $T \neq 0$ takes the form

$$S = \int \frac{d^2k}{(2\pi)^2} T \sum_{\sigma,\omega_n} [(i\omega_n - \zeta_{\mathbf{k}}) c_\sigma^\dagger(\mathbf{k}, \omega_n) c_\sigma(\mathbf{k}, \omega_n)$$

$$- \frac{\sigma}{2} \Delta_k c_\sigma^\dagger(\mathbf{k}, \omega_n) c_\sigma^\dagger(\textbf{-k}, -\omega_n) + h.c. + O(c^4) \tag{A2}$$

We thus just have to find the elements of matrix M by matching the corresponding terms in the two forms of action. Before doing that, we need to separate the sum over momenta into those over $\mathbf{k}$ and those over $\mathbf{k} - \mathbf{Q}$. Doing this, it can be checked that the action takes the form

$$S = \int \frac{d^2k}{(2\pi)^2} T \sum_{\omega_n} \sum_{n=1,2,a=1}^{N_f} \overline{\Psi}_{n,a}(\mathbf{k}, \omega_n)(i\omega_n - \zeta_k M_1 - \Delta_k M_2) \Psi_{n,a}(\mathbf{k}, \omega_n) \tag{A3}$$

where

$$M_1 = \begin{pmatrix} i & 0 & 0 & 0 \\ 0 & -i & 0 & 0 \\ 0 & 0 & i & 0 \\ 0 & 0 & 0 & -i \end{pmatrix}$$

$$M_2 = \begin{pmatrix} 0 & 1 & 0 & 0 \\ 1 & 0 & 0 & 0 \\ 0 & 0 & 0 & 1 \\ 0 & 0 & 1 & 0 \end{pmatrix} \tag{A4}$$

Note that the form of M_1 and M_2 is fixed by the form of kinetic energy ζ_k and the gap symmetry Δ_k respectively, and is therefore unique. These are expanded to lowest order as $\zeta_k \simeq v_F k_x$ and $\Delta_k \simeq \frac{8\Delta k_y^2}{k_F}$ for node 1 as example. The resulting effective action is not Lorentz invariant even if we try to rescale the coefficients in front of the operators in the bracketed terms. The first two terms in the bracket can however be treated as if they form a half-Dirac action and we can thus write the Dirac representation for these two terms which demands us to construct two anti-commutating 4×4 Dirac γ matrices. We can of course define another γ matrix, call it γ_2, for the third term but that is not bound to satisfying anti-commutation relation with the first two γ matrices. We choose the following representation;

$$\gamma_0 = \begin{pmatrix} 0 & 0 & 1 & 0 \\ 0 & 0 & 0 & -1 \\ 1 & 0 & 0 & 0 \\ 0 & -1 & 0 & 0 \end{pmatrix}$$

$$\gamma_1 = \begin{pmatrix} 0 & 0 & 1 & 0 \\ 0 & 0 & 0 & 1 \\ -1 & 0 & 0 & 0 \\ 0 & -1 & 0 & 0 \end{pmatrix}$$

$$\gamma_2 = \begin{pmatrix} 0 & 0 & 0 & 1 \\ 0 & 0 & -1 & 0 \\ 0 & 1 & 0 & 0 \\ -1 & 0 & 0 & 0 \end{pmatrix} \tag{A5}$$

The choice of γ_1 for the "Yukawa coupling" for interaction action in equation 3 is derived based on symmetry consideration as follows. The fermion-boson coupling action must clearly preserve C_4 symmetry of the theory since the theory must be invariant if we rotate the momentum space by $\frac{\pi}{2}$. Under this rotation, the operators in the 4×1 Nambu spinor in Eq.(4) transforms as

$$c_{1,a+}(\mathbf{k}, \omega_n) \rightarrow c_{2,a+}(\mathbf{k}, \omega_n) \rightarrow c_{1,a-}(-\mathbf{k}, -\omega_n)$$

$$c^{\dagger}_{1,a-}(-\mathbf{k}, -\omega_n) \rightarrow c^{\dagger}_{2,a-}(-\mathbf{k}, -\omega_n) \rightarrow c^{\dagger}_{1,a+}(\mathbf{k}, \omega_n)$$

$$c_{1,a+}(\mathbf{k} - \mathbf{Q}_1, \omega_n) \rightarrow c_{2,a+}(\mathbf{k} - \mathbf{Q}_2, \omega_n) \rightarrow c_{1,a-}(-\mathbf{k} + \mathbf{Q}_1, -\omega_n)$$

$$c^{\dagger}_{1,a-}(-\mathbf{k} + \mathbf{Q}_1, -\omega_n) \rightarrow c^{\dagger}_{2,a-}(-\mathbf{k} + \mathbf{Q}_2, -\omega_n) \rightarrow c^{\dagger}_{1,a+}(\mathbf{k} - \mathbf{Q}_1, \omega_n) \tag{A6}$$

With lengthy but otherwise straightforward algebra it can be verified directly that

$$S_{\psi\phi} = \lambda \int d^2x \int d\tau \sum_{n=1,a=1,2}^{N_f} \phi \overline{\Psi}_{n,a} \gamma_1 \Psi_{n,a} \tag{A7}$$

is invariant under this C_4 transformation, while other choices such as $S_{\psi\phi} = \lambda \int d^2x \int d\tau \sum_{n=1,a=1}^{N_f} \phi \overline{\Psi}_{n,a} \gamma_0 \Psi_{n,a}$ are not. Invariance under C_4 symmetry is the minimum symmetry requirement that must be satisfied by the action and therefore we adopt this particular choice of Yukawa coupling.

Appendix B: $\frac{1}{N_f}$ Self-energy Correction to Fermion Propagator and Yukawa Vertex Correction

We consider a theory of fermions with N_f flavors, written as 2×1 spinor which means we consider only one of the two nodes in each of $1\overline{1}$ and $2\overline{2}$ pairs, interacting with real scalar field through Yukawa coupling.

$$S_{\Psi} = \int \frac{d^2k}{(2\pi)^2} T \sum_{\omega_m} \sum_{a=1}^{N_f} \overline{\Psi}_{1,a}(-i\omega_m \tau^z + v_f k_x \tau^t + \frac{8v_{\Delta}}{k_F} k_y^2 i\tau^y)\Psi_{1,a} + \overline{\Psi}_{2,a}(-i\omega_m \tau^z + v_f k_y \tau^t + \frac{8v_{\Delta}}{k_F} k_x^2 i\tau^y)\Psi_{2,a} \tag{B1}$$

$$S_{\phi} = \int d^2x d\tau (\frac{1}{2}(\nabla\phi)^2 + \frac{1}{2}c^2(\partial_{\tau}\phi)^2 + \frac{1}{2}r\phi^2 + \frac{u}{4!}\phi^4) \tag{B2}$$

$$S_{\Psi\phi} = \lambda \int d^2x \int d\tau \phi \sum_{n=1,a=1}^{N_f} \overline{\Psi}_{n,a} \tau^t \Psi_{n,a} \tag{B3}$$

Here, the 2×1 Nambu spinor is given by

$$\Psi'^{\dagger}_{n,a}(\mathbf{k}, \omega_m) = (c^{\dagger}_{+n,a}(\mathbf{k}, \omega_m), c_{-n,a}(-\mathbf{k}, -\omega_m))$$

and $\overline{\Psi}_{n,a} = \Psi^{\dagger}_{n,a}\tau^t$, where ω_n is the Matsubara (imaginary, Euclidean) frequency of finite temperature T field theory for fermion given by $\omega_m = (2m+1)\pi T$ and $\tau^{x,y,z}$ are the usual Pauli spin matrices and τ^t is 2×2 identity matrix.

Let us now however consider the zero temperature $T = 0$ version of the same field theory in which the we convert the discrete Euclidean imaginary Matsubara frequency ω_m into continuous Minkowskian real frequency $\omega \equiv k_0$ by Wick rotation $i\omega_m \rightarrow \omega$ and the corresponding sum into integral. We now compute the one-loop Feynman diagram for fermion self energy given by the following Feynman diagrams;

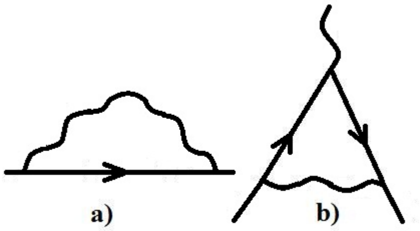

FIG. B1 One-loop Feynman diagrams for fermion self energy and Yukawa vertex

with the corresponding expressions,

$$\Sigma_{\Psi}^{1loop}(p) = \frac{1}{N_f}\int \frac{d^3k}{(2\pi)^3}\frac{i(p_0+k_0)\tau^z + v_F(p_1+k_1)\tau^t - \eta(p_2+k_2)^2 i\tau^y}{[(p_0+k_0)^2 + v_F^2(p_1+k_1)^2 + \eta^2(p_2+k_2)^4](r+\Gamma_2(k))} \tag{B4}$$

where $\Gamma_2(k)$ is the two-point function given in Eq. (8).

$$\Gamma_2(k) = 4\int \frac{d^3p}{(2\pi)^3}\frac{-\Omega(\Omega+\omega) + v_F^2 p_x(p_x+k_x) + \xi^2 p_y^2(p_y+k_y)^2}{((\Omega+\omega)^2 + v_F^2(p_x+k_x)^2 + \xi^2(p_y+k_y)^4)(\Omega^2 + v_F^2 p_x^2 + \eta^2 p_y^4)} + (x \leftrightarrow y) \tag{B5}$$

This is the fermion self energy correction from its coupling to bosonic Ising nematic scalar field. Note that we have not only the non-Lorentz p_2^2 term but also the Lorentz symmetry breaking $v_F \neq 1$ term even if we isolate the $i(p_0+k_0)\tau^z + v_F(p_1+k_1)\tau^t$ part and try to consider it as a $1+1$ Dirac action. The Yukawa vertex at zero external momenta-frequency is given by

$$\Xi(0) = \frac{1}{N_f}\int \frac{d^3p}{(2\pi)^3} Tr[\tau^t G_{\Psi}(p_x,p_y,\Omega)\tau^t G_{\Psi}(p_x,p_y,\Omega)\tau^t \frac{1}{r+\Gamma_2(p,\Omega)}) \tag{B6}$$

These two quantities were used to analyze the structure of RG equations of the theory (equations 1, 2 and 3) in Section III.

Appendix C: Details on Quasiparticle Spectral Function Calculation

Here we give the expression for the elements of quasiparticle self energy needed for the calculation of its spectral function in in Section IV. From

$$\Sigma_{\Psi}(k_x,k_y,\omega) = \lambda^2\int \frac{d^3p}{(2\pi)^3}\frac{i(\omega+\Omega)\gamma_0 - v_F(k_x+p_x)\gamma_1 - \eta(k_y+p_y)^2\gamma_2}{[(\omega+\Omega)^2 + v_F^2(k_x+p_x)^2 + \eta^2(k_y+p_y)^4](r+\Gamma_2(p))} \tag{C1}$$

where $\eta = \frac{8v_{\Delta}}{k_F}$ and λ is the fermion-nematic coupling constant in Eq.(3) which we recover here (rather than normalized to 1) in order to study the effect of nematic critical fluctuations on quasiparticle spectral function in Section IV. Using representation (4), we have

$$\Sigma^a(k_x,k_y,\omega) = \lambda^2\int \frac{d^3p}{(2\pi)^3}\frac{i(\omega+\Omega)}{[(\omega+\Omega)^2 + v_F^2(k_x+p_x)^2 + \eta^2(k_y+p_y)^4](r+\Gamma_2(p))} \tag{C2}$$

$$\Sigma^b(k_x,k_y,\omega)=\lambda^2\int\frac{d^3p}{(2\pi)^3}\frac{-v_F(k_x+p_x)}{[(\omega+\Omega)^2+v_F^2(k_x+p_x)^2+\eta^2(k_y+p_y)^4](r+\Gamma_2(p))} \tag{C3}$$

$$\Sigma^c(k_x,k_y,\omega)=\lambda^2\int\frac{d^3p}{(2\pi)^3}\frac{-\eta(k_y+p_y)^2}{[(\omega+\Omega)^2+v_F^2(k_x+p_x)^2+\eta^2(k_y+p_y)^4](r+\Gamma_2(p))} \tag{C4}$$

These expressions are used to obtain the quasiparticle spectral function shown in Fig. 7.

---

[1] P. M. Chaikin and T. C. Lubensky, Principles of Condensed Matter Physics (Cambridge University Press, 1995); S. A. Kivelson, E. Fradkin, and V. J. Emery, Nature (London) 393, 550 (1998).

[2] E.A. Kim, M.J. Lawler, P. Oreto, S. Sachdev, E. Fradkin, and S.A. Kivelson, Phys. Rev. B 77, 184514 (2008).

[3] Y. Huh and S. Sachdev, Phys. Rev. B 78, 064512 (2008).

[4] C. Xu, M. Muller and S. Sachdev, Phys. Rev. B 78, 020501 (2008).

[5] C. Xu and Y. Qi and S. Sachdev, Phys. Rev. B 78, 134507 (2008).

[6] Y. Qi and C. Xu, Phys. Rev. B 80, 094402 (2009).

[7] V. Oganesyan, S.A. Kivelson, and E. Fradkin, Phys. Rev. B 64, 195109 (2001).

[8] T.-M. Chuang et al.,Science 327, 5962 (2010).

[9] V. Stanev, B.S. Alexandrov, P. Nikolic, and Z. Tesanovic, Phys. Rev. B 84, 014505 (2011).

[10] R.M. Fernandes and J. Schmalian, Phys. Rev. B 84, 012505 (2011).

[11] M. Vojta, Y. Zhang , and S. Sachdev, Phys. Rev. Lett. 85, 4940 (2000); 100, 089904(E) (2008); Int. J. Mod. Phys. B 14, 3179 (2000); (2008), arXiv: 0008048v2.

[12] M. Vojta, Y. Zhang , and S. Sachdev, Phys. Rev. B 62, 6721 (2000).

[13] I. J. Pomeranchuk, Sov. Phys. JETP 8, 361 (1958).

[14] H. Yamase, V. Oganesyan, W. Metzner, Phys. Rev. B 72, 035114 (2005).

[15] H. Zhai, F. Wang, D-H. Lee, Phys. Rev. B 80, 064517 (2009).

[16] M. Norman, Physics 1, 21 (2008).

[17] W. Lv, J. Wu, and P. Phillips, Phys. Rev. B 80, 224506 (2009).

[18] S. Sachdev, Quantum Phase Transitions (Cambridge University Press, 1999).

[19] J. A. Hertz, Phys. Rev. B 14, 1165 (1976), A.J. Millis, Phys. Rev. B 48, 7183 (1993).

[20] J. Zinn-Justin, Quantum Field Theory and Critical Phenomena (Clarendon Press, Oxford, 1989).

[21] A. Pelissetto, S. Sachdev, and E. Vicari, Phys. Rev. Lett. 101, 027005 (2008).

[22] Jiangping Hu and Cenke Xu:arXiv:1112.2713v1.

[23] P.E. Lammert, D.S. Rokhsar, and J. Toner, Phys. Rev. Lett. 70, 1650 (1993).

[24] L. W. Harriger, H. Q. Luo, M. S. Liu, C. Frost, J. P. Hu, M. R. Norman, and Pengcheng Dai,Phys. Rev. B 84, 054544 (2011).

[25] T. A. Maier, S. Graser, D. J. Scalapino, and P. J. Hirschfeld, Phys. Rev. B 79, 224510 (2009).

[26] M. Khodas and A. V. Chubukov, Phys. Rev. B 86, 144519 (2012).

[27] B. I. Halperin and P. C. Hohenberg, Phys. Rev. 177, 952 (1969);Phys. Rev. Lett. 19, 940 (1967).

[28] P. C. Hohenberg and B. I. Halperin, Rev. Mod. Phys. 49, 435 (1977).

[29] T. Li and Q. Han, J. Phys.: Condens. Matter 23 (2011) 105603(5pp).